

# Early Diastolic Strain-Velocity Temporal Relationship Assessment Using SPAMM-PAVE

Z. Zhang<sup>1</sup>, D. P. Dione<sup>1</sup>, P. B. Brown<sup>1</sup>, E. M. Shapiro<sup>1</sup>, C. Wu<sup>2</sup>, R. T. Constable<sup>1</sup>, A. J. Sinusas<sup>1</sup>, and S. Sampath<sup>1</sup>

<sup>1</sup>Yale University School of Medicine, New Haven, CT, United States, <sup>2</sup>Yale University School of Public Health, New Haven, CT, United States

**Introduction:** The passive interaction between left ventricular (LV) myocardial deformation and intra-cavity hemodynamics during diastolic filling is reflective of the underlying variations in regional myocardial viscoelastic properties [1, 2], and key to the understanding of diastolic dysfunction in various disease states. These relationships have not yet been well characterized, partially due to a lack of a well-established measurement protocol [3, 4]. We present here a novel MR imaging technique, spatial modulation of magnetization with polarity alternated velocity encoding (SPAMM-PAVE), to provide simultaneous measurements of 1-D myocardial displacement and chamber blood velocity. This technique is extended from SPAMM n' EGGS [5], with temporal resolution optimized up to 15 ms, sensitive to dynamic early diastolic events undetectable by current state-of-the-art methods.

**Fig 1. Pulse Sequence Timing Diagram.** Tagging modulation and bipolar gradient pulses with changed polarity are highlighted by red boxes.

As shown in Fig. 1, a 1-1 SPAMM tag preparation, triggered by the R-wave of the QRST complex, is applied to provide sensitivity to tissue displacement. At the beginning of each heartbeat a delay  $D_1$  was inserted to limit the number of RF pulses for improved tag contrast during diastole. Within each main acquisition frame, bipolar gradient pulses sensitive to chamber blood velocity are played out with opposite polarity every alternate time frame. An EPI (center-out flyback with 3 echoes per segment) trajectory was used for data acquisition, and a 4-fold GRAPPA was implemented to minimize the scan time to a 19s breath-hold. Finally, a second delay,  $D_2$ , was employed to facilitate full recovery of the longitudinal magnetization to its steady-state. To maintain optimized tag contrast across all frames, a specialized train of incrementing flip angles  $\alpha_n$ ,  $\alpha_n = \text{atan}(\sin(\alpha_{n-1}) \cdot \exp(-TR/T_2)) + B(A-n)/A \cdot n$ , was applied, where n denotes the number of imaging RF pulses, B and A are the slope and intercept factors for the additive ramp-down function. The optimized A and B were experimentally determined as 0.5 and 0.25.

**Experiments and Results:** One normal (i.e., no prior diagnosis or symptoms of any heart disease) volunteer intra-subject study [male; age: 35 yrs; height: 1.82 m; weight: 180 kg] and 8 normal volunteer inter-subject studies [3 females, 5 males; age: 35.00 (8.81) (mean (SD)) yrs; height: 1.74 (0.09) m; weight: 76.60 (14.23) kg] were conducted on a 1.5 T Siemens Sonata scanner, with key parameters set as, imaging matrix: 192x192, resolution: 1.5mmx1.5mm, slice thickness: 8mm, views per cardiac phase: 3, TR: 14ms, tag separation: 8mm, Venc: 150 cm/s,  $\alpha_n$ : 15°,  $D_1$  and  $D_2$  were respectively of 35% and 10% of the R-R cycle. 2 long-axis slices, 2-chamber and 4-chamber views, were acquired for all volunteer studies. As an example, a series of intra-cavity blood velocity maps with a strain mask are illustrated in Fig.2 (a). Regions of interest of LV myocardial wall and mitral valve inflow were user-contoured according to a standard from American Society of Echocardiography's Guidelines, as shown in Fig. 2(b). Fig. 3 shows the mean time curves of longitudinal strain in basal, mid-cavity, and apical regions of anterior, inferior, septal and lateral LV wall from 8 subjects, in addition to averaged mitral valve inflow velocity curve. We define the rapid filling phase, composed of acceleration and deceleration of blood inflow, to be the time interval during which the velocity curve is above 5% of its maximum value. The end-systolic time frame, empirically defined in this study as 80 ms ahead of the onset of rapid filling, is used as the reference time-frame for the Lagrangian strain calculation. The strain-velocity curves reveal in great detail the time evolution of regional diastolic function during passive filling. From the regional strain curves, it can be observed that the apical region curves feature a relative high rate of longitudinal extension during and plateauing at the end of acceleration filling phase Acc. The basal region curves plateau at the end of the deceleration phase Dec. Such curves may shed insight into the interplay between regional volumetric changes in the left ventricle in response to filling patterns. Considering each time point of the acquisition as an independent measure, we also calculate the temporal Intraclass Correlation Coefficient (ICC<sub>t</sub>), which directly estimates the reliability of the strain measurement. High ICC<sub>t</sub> values of intra-subject study demonstrate the high reliability and repeatability of the SPAMM-PAVE measurement. Lower ICC<sub>t</sub> from inter-subject study is

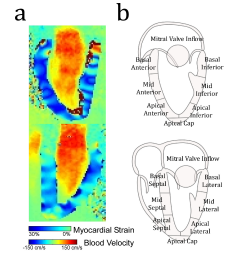


**Fig 2. (a) Color-coded velocity maps of 2- and 4-chamber views with tailored LV myocardial strain maps overlaid. (b) Standards for strain and flow segmentation.**

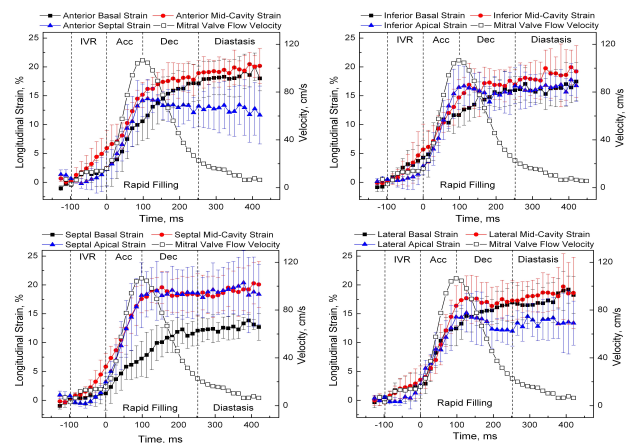


**Fig. 3. Time plots comparing the mean of averaged longitudinal strain and the mean of averaged mitral valve inflow blood velocity of the 8 subjects in basal, mid-cavity, and apical regions of anterior, inferior (top two), septal and lateral walls (bottom two). Standard deviation of each strain datum is illustrated as well. Strain-velocity interactions during diastolic phases of isovolumic relaxation (IVR), rapid filling (acceleration and deceleration), and early diastasis can be observed.**

	2 Chamber View						4 Chamber View					
	Anterior			Inferior			Septal			Lateral		
	Basal	Mid	Apical	Basal	Mid	Apical	Basal	Mid	Apical	Basal	Mid	Apical
<b>Intra-Subject</b>	0.931	0.970	0.924	0.935	0.961	0.974	0.916	0.926	0.945	0.927	0.956	0.921
<b>Inter-Subject</b>	0.766	0.826	0.718	0.758	0.826	0.785	0.714	0.819	0.752	0.825	0.786	0.743

**Table 1. ICC<sub>t</sub>. Describing the reliability of SPAMM-PAVE measurement with frames.**

from the individual difference in strain values, as predicted.

**Conclusion:** SPAMM-PAVE is a reliable technique, and shows great potential to comprehensively characterize diastolic passive strain-velocity relationships in the left ventricle at high temporal resolutions, and may bear significance in identifying diastolic functional abnormalities.

**Reference:** 1. Zile MR, et. al., Circulation. 2002 Mar; 105:1387-1393. 2. Claessens TE, et. al., Ultrasound Med Biol. 2007 Jun;33:823-841. 3. Wen H, et. al., Magn Reson Med 2005; 54: 538-548. 4. Thompson RB, et. al., Magn Reson Med. 2002 Mar;47(3):499-512. 5. Sampath S, et. al., J Magn Reson Imaging 2008; 27: 809-817.